ChemComm

COMMUNICATION

View Article Online
View Journal | View Issue

Cite this: *Chem. Commun.*, 2023, 59, 9884

Received 19th June 2023,
Accepted 20th July 2023

DOI: 10.1039/d3cc02938g

rsc.li/chemcomm

Selective adsorption of dihydrogen isotopes on DUT-8 (Ni,Co) monitored by *in situ* electron paramagnetic resonance†

Muhammad Fernadi Lukman,[a] Matthias Mendt,[b] Volodymyr Bon,[c] Stefan Kaskel[c] and Andreas Pöppl*[a]

In situ **continuous wave electron paramagnetic resonance investigation has been proven as a powerful method by employing paramagnetic Ni^{2+}–Co^{2+} pairs as spin probes to follow the isotope-selective gate opening phenomenon on the DUT-8($Ni_{0.98}$ $Co_{0.02}$) framework. This method is very sensitive to detect the phase transition from the closed pore to the open pore phase in response to D_2 adsorption in the framework, while no phase transformation has been observed during H_2 gas adsorption. More interestingly, it is also able to sense local structural changes around the spin probe during the desorption of D_2 gas. Based on these evidences, the *in situ* continuous wave electron paramagnetic resonance method can be implemented as an efficient and non-invasive technique for the detection of dihydrogen isotopes.**

Flexible metal organic frameworks such as MIL-53(Al) and DUT-8(Ni) are considered as very attractive MOFs due to their switchability behaviour towards external stimuli such as the adsorption of specific guest molecules, pressure or temperature.[1–5] Recently, Kim and co-workers[6] reported a D_2-selective breathing behaviour in MIL-53(Al), which is potentially useful for the purification of isotopic mixtures. In addition, some of us also revealed that a flexible DUT-8(Ni) selectively responds to D_2 gas, while in a contrasting way, is irresponsive towards HD and H_2 gas.[7] The flexible DUT-8(Ni) MOF is a primitive cubic (**pcu**) network that consists of Ni_2 paddle wheels as nodes (see Fig. 1), 2,6-naphthalenedicarboxylate (ndc) as a linker and 1,4-diazabicyclo-[2,2,2]octane (dabco) as pillars. A pronounced nuclear quantum effect[8–11] is suggested to be responsible for the higher adsorption enthalpy of deuterium-containing dihydrogen isotopes to be adsorbed inside the DUT-8(Ni) framework at cryogenic temperatures.

Previously, *in situ* neutron powder diffraction (NPD) and thermal desorption spectroscopy (TDS) investigations were conducted to study this intriguing effect demonstrating a high adsorption selectivity for D_2 *vs.* H_2 after exposure to 1 : 1 gas mixtures.[7]

On the other hand, from the point of view of electron paramagnetic resonance (EPR) spectroscopy, the isomorphous substitution of Co^{2+} towards DUT-8 (Ni) has been investigated and comprises a noticeable EPR pattern for an open pore (*op*) phase species that can be interpreted as an effective spin $S = 1/2$ ground state of the antiferromagnetically coupled mixed Ni^{2+}–Co^{2+} paddle wheel unit interacting with its ^{59}Co nuclear spin ($I = 7/2$).[5,12] A lengthy discussion on other possible assignments of EPR spectra for the *op* phase state and its rejection arguments has been discussed by Ehrling and co-workers.[5] Previously, an *in situ* CW-EPR approach enabled us to follow the gate opening mechanism for a series of DUT-8($Ni_{1-x}Co_x$) samples in response to their exposure to N_2 gas close to its standard boiling point (71 K).[12] Even preceding that, the exotic *in situ* CW-EPR investigation at X-band frequency has been

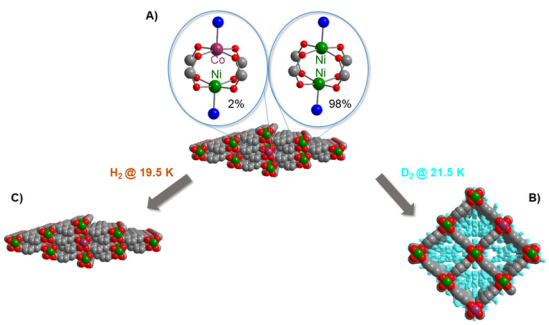

Fig. 1 (A) Structural representation of mixed-metal Ni^{2+}–Co^{2+} paddle wheel units. Blue, grey and red spheres indicate nitrogen, carbon and oxygen atoms, respectively. A schematic representation of the (B) *op* phase and (C) *cp* phase state in response to dihydrogen isotope adsorption is also provided.

[a] *Felix Bloch Institute for Solid State Physics, Leipzig University, 04103 Leipzig, Germany. E-mail: poeppl@physik.uni-leipzig.de*
[b] *SaxonQ GmbH, Emilienstr. 15, 04107 Leipzig, Germany*
[c] *Chair of Inorganic Chemistry I, Technische Universität Dresden, 01069 Dresden, Germany*

† Electronic supplementary information (ESI) available. See DOI: https://doi.org/10.1039/d3cc02938g

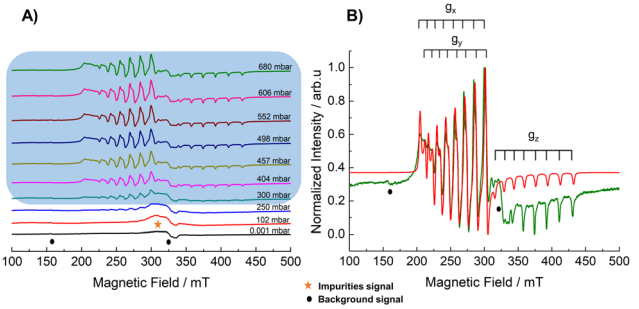

Fig. 2 (A) *In situ* CW-EPR spectra of DUT-8($Ni_{0.98}$ $Co_{0.02}$) while adsorbing D_2 gas from p = 0.001 mbar (black) to p = 680 mbar (green) recorded at 21.5 K. The impurity signal marked with a yellow star is tentatively assigned to some low spin Co^{2+} defect species while the black circle indicates a background signal from the cryostat. (B) The CW-EPR spectra of Ni^{2+}–Co^{2+} of species A representing the *op* phase state of DUT-8($Ni_{0.98}$ $Co_{0.02}$) in response to D_2 adsorption recorded *in situ* at p = 680 mbar and T = 21.5 K (green lines) and its simulated spectra (red lines). Two black circles at magnetic fields of 150 and 340 mT indicate again a background signal from the cryostat.

implemented as a versatile method to follow the gate opening phenomenon of several flexible MOFs triggered by the response toward guest molecule stimuli.[12–16] In the present work, we implement this *in situ* CW-EPR technique for the first time to monitor an isotope-selective phase transition of DUT-8($Ni_{0.98}$ $Co_{0.02}$) towards dihydrogen isotopes.

Initially, there was no signal observed for DUT-8($Ni_{0.98}$ $Co_{0.02}$) in the evacuated state (*ca.* 10^{-4} mbar), which indicates the presence of closed pore (*cp*) phase at 21.5 K, in agreement with previous results.[5,12] The absence of an EPR signal is probably due to short relaxation times of low symmetric Ni^{2+}–Co^{2+} paddle wheels. The spectral pattern distinctly evolved after increasing the D_2 pressure to 250 mbar, producing a nicely resolved species A (see Fig. 2A and Table 1 for the spin Hamiltonian parameters), which is assigned to the Ni^{2+}–Co^{2+} paddle wheel signal in the *op* phase state of DUT-8($Ni_{0.98}$ $Co_{0.02}$). The spin Hamiltonian parameters were determined by spectral simulation of the experimental EPR spectra. The intensity of species was obtained by double integration of the corresponding EPR spectra in Fig. 2A and served as a measure for the volume fraction of the *op* phase in the sample (Fig. 4). The emergence of the EPR spectrum of the Ni^{2+}–Co^{2+} paddle wheels at 250 mbar as an indication of the *op* phase is very well in line with the volumetric D_2 adsorption data obtained by Bondorf and co-workers,[7] where they also found a similar gate opening pressure and shape of the adsorption hysteresis for D_2 but with much longer equilibration times per pressure point.

Interestingly, after desorption to pressures less than 90 mbar, there is a gradual transformation of species A into a new species B with axial symmetry as presented in Fig. 3A (the percentage of its respective species is tabulated in Table SI1, ESI†). Its spectral pattern at 0.001 mbar is shown in Fig. 3B. The transformation of the symmetry of the paddle wheel units from lower symmetry into higher symmetry (C_4 as principal rotational axis) at low partial pressure of D_2 (p < 35 mbar) indicates less distortion for the paddle wheel units during the evacuation of D_2 gas. This phenomenon might originate from the adaptive response of the DUT-8($Ni_{0.98}$ $Co_{0.02}$) framework towards a D_2 release *via* a switching of the linker orientation and can subsequently change the symmetry into a more ordered state.[5,17]

The sensitivity of the EPR experiment allows one to observe such phase transformation in rather shorter timescales as compared to the volumetric D_2 and NPD measurements, which were previously published.[7] Note that the intensity of the EPR signal (considering double integration of species A which then transformed into species B) was observed to be constant during the desorption stage and did not revert back to the *cp* phase at least within the observation times of our EPR measurements (Fig. 4).

Desorption studies of D_2 with variability of time shown in Fig. SI3 (ESI†) indicated that even up to 33 minutes during pumping off at 0.001 mbar and 21.5 K, the *op* phase (*e.g.* Species B) is still observed with relatively constant EPR intensities. This supports the *in situ* NPD finding that the transition from *op* phase to *cp* phase would only be triggered after 24 h evacuation of D_2 at similar temperature (*ca.* 23.3 K).[7] One possible explanation might be that D_2 molecules are kinetically trapped in the pores since the dimension of the *cp* phase (2.366 nm × 0.695 nm) structure may accommodate the residual D_2 gas that was trapped during transition from the *op* to *cp* phase state. Pollock and co-workers[18] previously observed this trapping mechanism during the desorption of D_2 gas on

Table 1 Spin Hamiltonian parameters of the Ni^{2+}–Co^{2+} mixed paddle wheel species during the adsorption and desorption process of D_2. Ref. 12 refers to N_2 adsorption on the same sample as the reference. The hyperfine coupling is given in MHz

Species	g_x	g_y	g_z	A_x	A_y	A_z	Symmetry
A	2.65(4)	2.59(4)	1.79(4)	510(10)	465(10)	417(10)	Rhombic
B	2.62(4)	2.62(4)	1.80(4)	468(10)	468(10)	427(10)	Axial
12	2.62(4)	2.62(4)	1.39(4)	538(100)	538(100)	410(100)	Axial

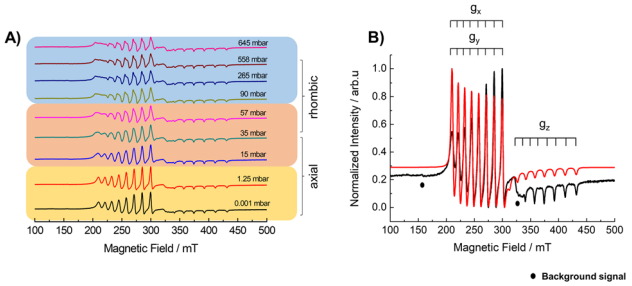

Fig. 3 (A) *In situ* CW EPR spectra of DUT-8($Ni_{0.98}$ $Co_{0.02}$) while desorbing D_2 gas from p = 645 mbar (pink) to p = 0.001 mbar (black). The orange shaded area indicates the superposition of rhombic Ni^{2+}–Co^{2+} species A and axial Ni^{2+}–Co^{2+} species B. The yellow shaded area indicates a complete transformation to the axial Ni^{2+}–Co^{2+} species B. *In situ* CW EPR signal for species B recorded after desorption of D_2 at 0.001 mbar and T = 21.5 K (black lines) with the simulated spectrum (red lines). Two black circles at magnetic field of 150 and 340 mT indicate a background signal from the cryostat.

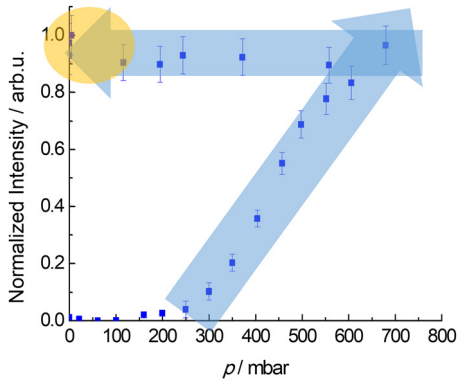

Fig. 4 Plot of EPR signal intensity of Ni^{2+}–Co^{2+} species for DUT-8($Ni_{0.98}$ $Co_{0.02}$) normalized with the highest EPR intensity during adsorption and desorption stages (blue shaded arrows).

another variant of flexible MOF material, MIL-53(Al), even at higher temperature (77 K). Moreover, this molecular clamp appeared to be functional until 120 °C when probed using neutron scattering measurements. We also attempted to increase the temperature while desorbing the D_2 gas under vacuum at 0.001 mbar, which resulted in a pore closing mechanism being triggered at 30 K (Fig. SI3, ESI†). The EPR spectra at that temperature suffered from intensity reduction and line broadening before vanishing at $T > 35$ K, leaving only the background signal. This result is in agreement with previous TDS results that observe the largest D_2 desorption peak between 25–30 K, which implies that the desorption temperature plays an important role in the gate closing mechanism in the DUT-8 (Ni) materials.

In the case of H_2 adsorption and desorption on DUT-8($Ni_{0.98}$ $Co_{0.02}$) at 19.5 K, which are provided in Fig. SI1 and SI2 (ESI†), the EPR intensities are constant and show only a low-spin Co^{2+} impurity signal together with some background signals from the cryostat (Fe^{3+} and Cu^{2+} species around 150 and 325 mT, respectively). This result signifies that the *op* phase with its characteristic EPR signal of the Ni^{2+}–Co^{2+} paddle wheel signal is not present within the pressure range of $0 \leq p \leq 929.2$ mbar during the H_2 adsorption experiment. However, it cannot be ruled out that a trace amount of H_2 gas is adsorbed in the *cp* phase without triggering a pore transition, simply because the energy barrier for the pore transformation is too high for H_2 at 19.5 K and pressures up to 1000 mbar.[7] The selective opening of DUT-8($Ni_{0.98}$ $Co_{0.02}$) towards D_2 owing to the so-called "sizable" chemical affinity quantum sieving (CAQS) effect originates from a slightly lower ZPE (zero point energy) that allows D_2 to bind preferentially to various adsorption sites, such as accessible paddle wheel units or linker sites.[7,10,19] We should note that the definition of the CAQS effect is not merely constrained to the adsorption of gases in the framework that poses open binding sites. Savchenko and co-workers[20] reported that the selectivity of D_2 over H_2 is mainly caused by different adsorption enthalpies, which in principle, is rooted fundamentally to the small difference in ZPE of adsorbed dihydrogen isotopes on the funnel-like, metal and linker sites in the MOF MFU-4l (at 50 K) where none of them can be considered as open sites in a straightforward definition.

In conclusion, we have demonstrated that the *in situ* CW-EPR technique at X-band frequencies can be implemented as an efficient technique to monitor the selective-adsorption of dihydrogen isotopes on DUT-8($Ni_{0.98}$ $Co_{0.02}$) MOF, which further confirms the isotope-selective phase transition in response to D_2 adsorption. Moreover, as an outlook, the utilisation of *in situ* pulsed-EPR techniques is in progress to locate the D_2 position with respect to the spin probe within the framework of DUT-8($Ni_{0.98}$ $Co_{0.02}$) and estimate how this gas interacts around the accessible paddle wheel units where our EPR active probe resides. This detailed information would provide more clarity in terms of understanding the nature of adsorption sites of the flexible MOF materials.

Muhammad Fernadi Lukman: conceptualization, methodology, investigation, data curation, writing – original draft, and writing – review & editing. Matthias Mendt: investigation, writing – review & editing. Volodymyr Bon: writing – review & editing. Stefan Kaskel: review and supervision. Andreas Pöppl: conceptualization, review, project administration, funding acquisition and supervision.

The authors would like to acknowledge the DFG funding of GRK 2721: Hydrogen Isotopes 1, 2, 3 H with project number 443871192 and FOR 2433 with project number 279409724.

Conflicts of interest

There are no conflicts to declare.

References

1 N. Klein, H. C. Hoffmann, A. Cadiau, J. Getzschmann, M. R. Lohe, S. Paasch, T. Heydenreich, K. Adil, I. Senkovska, E. Brunner and S. Kaskel, *J. Mater. Chem.*, 2012, **22**(20), 10303–10312.
2 Y. Liu, J. H. Her, A. Dailly, A. J. Ramirez-Cuesta, D. A. Neumann and C. M. Brown, *J. Am. Chem. Soc.*, 2008, **130**(35), 11813–11818.
3 M. I. Breeze, G. Clet, B. C. Campo, A. Vimont, M. Daturi, J. M. Grenèche, A. J. Dent, F. Millange and R. I. Walton, *Inorg. Chem.*, 2013, **52**(14), 8171–8182.
4 F. M. Mulder, B. Assfour, J. Huot, T. J. Dingemans, M. Wagemaker and A. J. Ramirez-Cuesta, *J. Phys. Chem. C*, 2010, **114**(23), 10648–10655.
5 S. Ehrling, E. M. Reynolds, V. Bon, I. Senkovska, T. E. Gorelik, J. D. Evans, M. Rauche, M. Mendt, M. S. Weiss, A. Pöppl, E. Brunner, U. Kaiser, A. L. Goodwin and S. Kaskel, *Nat. Chem.*, 2021, **13**(6), 568–574.
6 J. Y. Kim, J. Park, J. Ha, M. Jung, D. Wallacher, A. Franz, R. Balderas-Xicohténcatl, M. Hirscher, S. G. Kang, J. T. Park, I. H. Oh, H. R. Moon and H. Oh, *J. Am. Chem. Soc.*, 2020, **142**(31), 13278–13282.
7 L. Bondorf, J. L. Fiorio, V. Bon, L. Zhang, M. Maliuta, S. Ehrling, I. Senkovska, J. D. Evans, J.-O. Joswig, S. Kaskel, T. Heine and M. Hirscher, *Sci. Adv.*, 2022, **8**(15), 7035.
8 H. Oh and M. Hirscher, *Eur. J. Inorg. Chem.*, 2016, 4278–4289.
9 J. Y. Kim, H. Oh and H. R. Moon, *Adv. Mater.*, 2019, **31**, 1805293.
10 H. Oh, I. Savchenko, A. Mavrandonakis, T. Heine and M. Hirscher, *ACS Nano*, 2014, **8**(1), 761–770.
11 J. Y. Kim, J. Park, J. Ha, M. Jung, D. Wallacher, A. Franz, R. Balderas-Xicohténcatl, M. Hirscher, S. G. Kang, J. T. Park, I. H. Oh, H. R. Moon and H. Oh, *J. Am. Chem. Soc.*, 2020, **142**(31), 13278–13282.
12 S. Ehrling, M. Mendt, I. Senkovska, J. D. Evans, V. Bon, P. Petkov, C. Ehrling, F. Walenszus, A. Pöppl and S. Kaskel, *Chem. Mater.*, 2020, **32**(13), 5670–5681.

13 D. M. Polyukhov, S. Krause, V. Bon, A. S. Poryvaev, S. Kaskel and M. V. Fedin, *J. Phys. Chem. Lett.*, 2020, **11**(15), 5856–5862.
14 V. Bon, E. Brunner, A. Pöppl and S. Kaskel, *Adv. Funct. Mater.*, 2020, **30**(41), 1907847.
15 M. Mendt, P. Vervoorts, A. Schneemann, R. A. Fischer and A. Pöppl, *J. Phys. Chem. C*, 2019, **123**(5), 2940–2952.
16 K. Thangavel, F. Walenszus, M. Mendt, V. Bon, S. Kaskel and A. Pöppl, *J. Phys. Chem. C*, 2023, **127**(17), 8217–8234.
17 H. Miura, V. Bon, I. Senkovska, S. Ehrling, S. Watanabe, M. Ohba and S. Kaskel, *Dalton Trans.*, 2017, **46**(40), 14002–14011.
18 R. A. Pollock, J. H. Her, C. M. Brown, Y. Liu and A. Dailly, *J. Phys. Chem. C*, 2014, **118**(31), 18197–18206.
19 J. Teufel, H. Oh, M. Hirscher, M. Wahiduzzaman, L. Zhechkov, A. Kuc, T. Heine, D. Denysenko and D. Volkmer, *Adv. Mater.*, 2013, **25**(4), 635–639.
20 I. Savchenko, A. Mavrandonakis, T. Heine, H. Oh, J. Teufel and M. Hirscher, *Microporous Mesoporous Mater.*, 2015, **216**, 133–137.